MENG 473a **Project Report**
Special Projects II **20 December 2017**

To Move or Not to Move: Principal Curvatures of Articular Surfaces

Aaron West

Adviser: Dr. Madhusudhan Venkadesan

Abstract

When recreating species that no longer exist, paleontologists aim to put together bone structures to try to determine how that species may have moved. We aim to quantify their work by producing a geometric theory that can determine how a limb moves based on the surface geometry at its joint. Previous work has concluded that the movement in joints is determined by the surface geometry of adjoining bones and the attachment pattern of surrounding ligaments. However, we believe by producing a predictive geometric model we can determine joint displacement purely based on the principal curvatures of the articular surfaces of the joint. We aim to design an experiment that will allow us to predict movement capabilities at a joint based purely on the principal curvatures of the articular surfaces. To do this we have designed an experiment that will be used on a chicken knee bone. The experiment incorporates three key principles. First, we will apply a known displacement to one end of the bone. Second, we will measure a force at the other end. Third, we will rotate the joint about its neutral axis, and repeat displacement and measurements until we have data about all 360 degrees of the joint. With these three key principles, we can use Hooke's Law to determine stiffness at a given orientation, and ultimately determine which directions are the soft and stiff directions of the bone. Afterwards, this data can be compared to CT scans of the joint, which will be used to create a geometrical relationship between surface curvature and displacement.

Acknowledgements

Thank you to Professor Beth Anne Bennett, Glenn Weston-Murphy for your support with the MENG 474 Special Projects II course.

Thank you to Nick Bernardo for the countless hours of help and expertise in the machine shop.

Thank you to Kevin Ryan for your electronics expertise and help in setting up the linear rail guide.

Thank you to Madhusudhan Venkadesan, Neelima Sharma, and Ali Yawar for continuous help and guidance throughout the semester.

Table of Contents

INTRODUCTION

We have aimed to design an experiment that will test the theory that the displacement in a joint can be determined based purely on the principal curvatures at its articular surfaces. This experiment is part of the broader efforts to create a geometrical model that can relate surface geometry to displacement. To validate this work, we needed to answer two questions: Have other scientists tried to relate shape, or surface geometry, to joint stiffness? If so, what apparatus have they used in doing so?

In 2006, Santos and Valero-Cuevas investigated whether a single parametric kinematic model can represent all thumbs, in spite of the variance of thumb anatomy from person to person. Their work furthered the question on whether or not a single biomechanical model can represent the entire population. They found that anatomical and functional variability can be captured by a finite set of model-types [12]. Similarly, Grood and Suntay (1983) presented a joint coordinate system that provides a simple geometric description of the three-dimensional rotational and translational motion between two rigid bodies [6]. This work fits nicely into our work as it lays a foundation for the need of an experiment to automatically record joint data.

As mentioned before, we aim to design an experiment that can determine a joints soft and stiff directions. To do this, we will likely draw from the foundation laid by Grood and Suntay and Santos and Valero-Cuevas. However, what the latter brought forth was the need to tackle the problem of multiple degrees of freedom. Particularly, in our experiment we aim to have 5 free degrees of freedom and one imposed motion. Van Veen (2013) may have helped us address this problem by creating a planar ferrofluid bearing [14]. However, this planar bearing uses PWM to precisely position a stage, and in our experiment, we want to allow for free movement in a planar stage.

Many before us have used fossils to recreate species that no longer exist. Notably, Hutchinson and Carrano (2002) have used inference to relate the pelvic and hindlimb fossils of the Tyrannosaurus Rex to determine how that species formerly moved [4]. Currently, software exists to measure bone geometry [3] [5]. BoneJ, developed by Doube et al. (2010), is primarily designed to measure bone geometry. However, it does not yet have an application to relate this bone geometry to motion. Brainerd et al. (2010) has set out to use a set of 3D X-ray motion analysis techniques to relate motion data from in vivo X-ray videos to skeletal morphology data from bone scans. Their work is very promising in its analysis of creating a correlation between morphology and motion. However, its limiting factor is that they must be able to take motion data. For our purposes, this may not be feasible, as we want to do work similar to that of Hutchinson and Carrano and be able to recreate nonexistent species based purely on the fossils they left behind.

Work has been done to understand the kinematics of the glenohumeral joint [7] [8]. Specifically, Kelkar et al. (2001) used stereophotogrammetry to compare surface geometry of the joint to its kinematics. Karduna et al. (1996) investigated key factors that control shoulder motion using a magnetic tracking device. While both of these experiments led to telling arguments about the key factors in surface geometry that were important in various translations and rotations of the glenohumeral joint, neither created definitive conclusions that can be used to relate a particular surface geometry to the kinematics of a joint unrelated to the shoulder. It is in this knowledge gap where our work can be useful, as we aim to create a geometrical model that can relate surface geometry to displacement.

While this work is mostly theoretical, it has proven applications in the medical fields, specifically in the use of prosthetics. The medical profession has used prosthetic devices for years to replace defective natural joints [1]. One of the leading forms of biomedical research today is in biomechanics and prosthetics. Prostheses have expanded from the simple joint replacement to the replacement of many other organs such as endoluminal replacements [2]. Many methods have been proposed to recreate anatomically correct prostheses, but we believe one limitation is the lack of fundamental knowledge of the complex geometries of the various bones throughout the body. This work has the potential to bridge that knowledge gap.

The last motivation comes in the form of pure scientific curiosity. When recreating species that no longer exist, paleontologists aim to put together bone structures to try to determine how that species may have moved. This has even further implications in studying how that species may have gone about their daily life. We are not alone in this work. Marzke et al. [10] [11] has aimed to quantify the differences in curvature of the thumbs of living and fossil primates. His work has shown that the difference in thumb curvature between humans and our early ancestors may be a result of the increased tool use of the modern age.

In this report, we will give a background of the definitions of stiffness and ligaments, as they will be used throughout the paper. With an understanding of the background, we can move on to the process of designing this experiment. In the design section, you will be introduced to three key principles that will be referenced throughout the paper. Then, we will talk about the design constraints, namely degrees of freedom. Then, we will discuss how we addressed those design constraints in the first prototype. Then we will, introduce a few takeaways from the first prototype and introduce the final design. Following the design section of the paper, will be an experiments section which will explain the proof of concept experiments we attempted to run using a Lego hinge. Lastly, we will finish with a brief summary and suggestions for the next steps of this project.

BACKGROUND

In this section, we will give an overview of ligaments and stiffness, as it will be useful to understand these two terms in the context of this paper.

Ligaments

Ligaments are the fibrous connective tissues that connects a bone to another bone, forming a joint [9]. Ligaments are not to be confused with tendons that connect muscles to other muscles. Ligaments have a Young's modulus of about 30 MPa, and in our body are often used to control displacement of the joint. Ligaments are viscoelastic, meaning that they can resist deformation but can also return back to their original state after being deformed. When mentioning ligaments, it is also important to mention the purpose of the synovial membrane. It serves as a frictionless surface in between two bones that prohibits wear from constant surface contact as two bones move along one another at their joint. Together, ligaments and the synovial membrane allow for the everyday movements joints exhibit with minimal wear and tear. However, we aim to provide evidence that ligaments are not responsible for determining how a joint displaces. Rather, it is there to support the geometrical features that determine joint displacement.

Stiffness

Stiffness is the resistance of a member against deformation [13]. It is most commonly thought of in the context of a spring and can be mathematically understood using Hooke's Law, F = kx, where *k* is the spring constant, or stiffness, *F* is an applied force, and *x* is a measured displacement. In this paper stiffness will be used in a biological context. To help understand this, we shall use the knee as an example. When walking, the knee bends in the sagittal plane. This is done very naturally and with every step. Both the ligaments and articular surfaces in the knee (shown if Figure 1) allow for this kind of motion. This direction will be referred to in this paper as the soft direction. On the other hand, when trying to bend the knee along the coronal plane, one faces a lot of resistance. In fact, this sort of motion is what causes many knee injuries, such as an ACL tear. There is high resistance against deformation in this direction. Throughout this paper, we will refer to a direction similar to this one as the stiff direction.

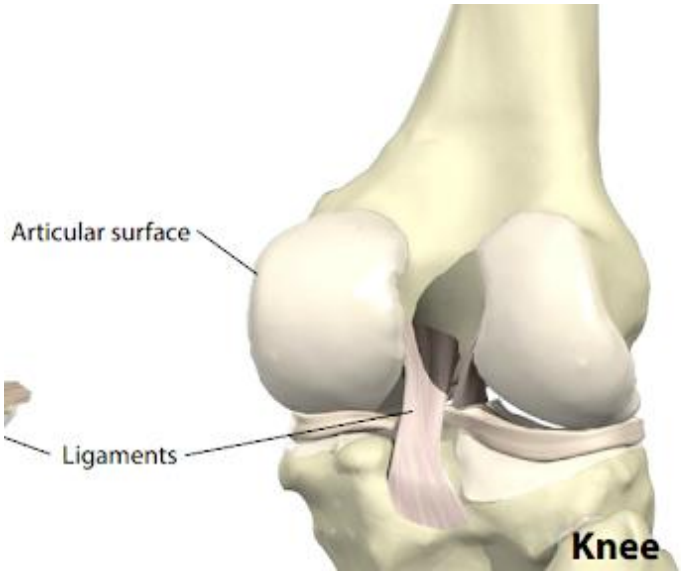

Figure 1: *In this picture of the knee, you can see the bones that surround the knee and the ligaments that connect these bones. We want to emphasize the articular surfaces, which are the surfaces of each bone that touch one another and form the joint. The ligaments are the fibrous tissues that hold the bones together, and can be seen in this picture.*

DESIGN

This project was completed over the course of two semesters. In the first semester many of the design constraints were realized and addressed in the first prototype. Many iterations were gone through before reaching this prototype. However, to produce a more concise paper we will show you the first prototype and then the final design.

Our project was split in two directions: first, we aimed to design the experiment; second, we sought a 'proof of concept' and thus ran experiments with a joint of known soft and stiff directions. In this section, we will first touch on the process of designing the experiment. Particularly, we will introduce you to the 3 key principles of our design and the biggest design constraints that we realized last semester. Then we will show you the first prototype that was produced last semester and how it addressed those 3 key principles and design constraints. With knowledge of that work we can began to introduce you to what we realized where the next steps and would be the starting point of the work

done this semester. That will be talked about in the takeaways section. Lastly, we will introduce you to the final design. Thereafter, we give a more detailed description of our 'proof of concept' experiments.

Key Design Principles

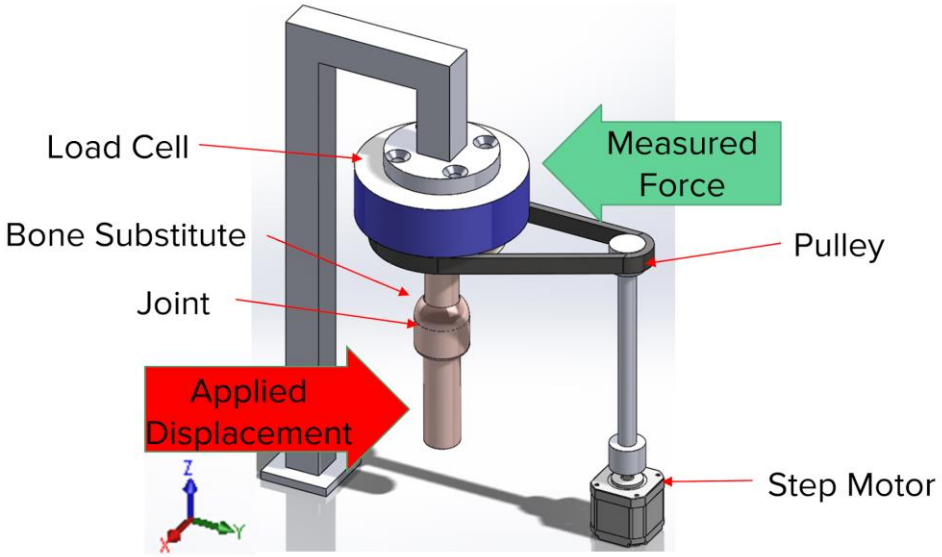

Figure 2: An isometric Solidworks screenshot of the earliest design iteration. In this figure, we can see the blue load cell used to measure force, the bone substitute and joint in the pink, flesh-like color, a stepper motor in grey, and a pulley in black.

As mentioned earlier, the aim of this project is to test the theory that one can determine the displacement of a bone purely based on the principal curvatures of the articular surfaces of the joint. In Figure 2 above, you will see a Solidworks screenshot of the earliest design iteration. In this figure, you can see the blue load cell used to measure force, the bone substitute and joint in the pink, flesh-like color, a stepper motor in grey, and a pulley in black. From this figure, three very important design considerations are displayed that will dictate how we approach the rest of the design process. The 3 key principles are:

1. Applied displacement
2. Measured force
3. Rotation of the bone in between measurements

The first key aspect is the applied displacement highlighted by the red arrow on the bottom left. The initial thought process was that on this free end of the joint, we would apply a specific, repeatable displacement. This displacement would be our control variable. From this displacement comes our second key aspect, the measured force at the load cell, denoted by a green arrow. With this measured force, using statics, one can determine the stiffness of the joint itself. However, this is only in one particular orientation, which brings us to the third key aspect: rotation of the bone in between measurements, which can be seen by the pulley and the attached stepper motor. Specifically, one will apply a displacement, and then measure a force for one orientation. Then the joint will be rotated some

increment of degrees about the z-axis. At this new orientation the same displacement will be applied and more force data will be measured. Ultimately this process will be repeated for 360 degrees. Then, we will know all the soft and stiff directions of the bone. Ultimately, we can compare the stiffness data to CT scans of the bone and create a mathematical correlation between surface geometry and stiffness.

Design Constraints

Unfortunately, there were a few key flaws in the early design. We did not accurately account for the degrees of freedom. For simplification of calculations, we wanted to have one imposed motion, displacement, of the bone. All the other 5 degrees of motion should be free. When this is the case, we can quite easily correlate the applied displacement and the measured force to a stiffness value, using equation 1 below,

$$k = \frac{dx}{dF} \quad (1)$$

where *k* is the calculated stiffness, *dx* is the displacement, and *dF* is the change in force. This equation is similar to that of Hooke's Law, F=kx. However, we are assuming that the ligament attached to our joint is not a linear spring. Thus, we must use the change of force and the change of displacement from the neutral position to obtain a relative stiffness in that specific orientation.

Moving forward we chose the degrees of freedom to include rotation about the x-axis, rotation about the y-axis, rotation about the z-axis, translation along the x-axis, and translation along the y-axis. The imposed displacement would be translation along the z-axis.

Figure 1 did not satisfy these design constraints. In this design, we aimed to add the displacement along the y-axis. However, there was no apparatus to ensure that the displacement was added purely in the y-direction. For example, take a rolled piece of paper and try to displace it with your finger in one direction. It is likely that you observed slipping. This occurs when your finger is not directly perpendicular to the surface you were pushing on. Friction has allowed you finger to move out of the line with the intended perpendicular direction. Thus, you have now imposed a motion in two directions, and now you have two controlled variables instead of one. Additionally, since this slipping is not repeatable in every direction of the bone, you are likely not displacing the bone in a repeatable fashion. Thus, the experiment has loss accuracy.

First Prototype

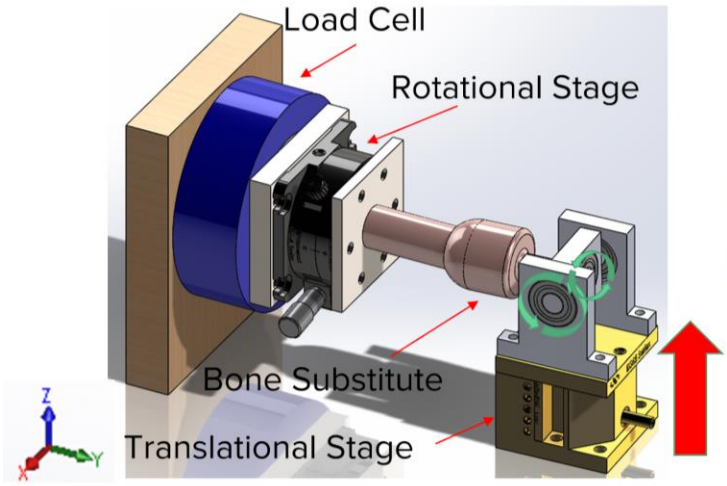

(a)

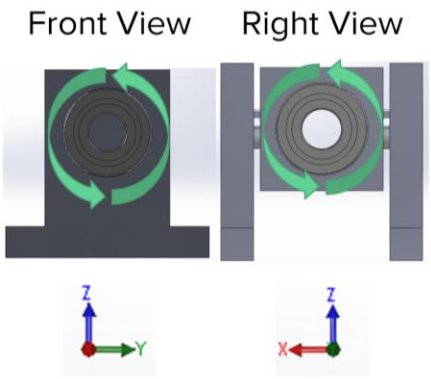

(b)

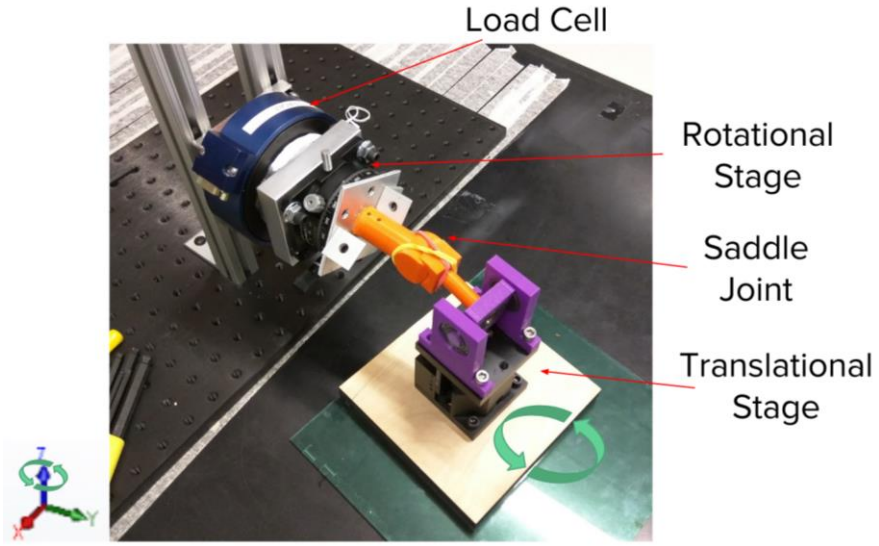

(c)

Figure 3: (a) An isometric Solidworks screenshot of the third design iteration. In the blue is a load cell used to measure force. In the grey next the load cell is a high-flatness plate used to connect the load cell to the black Newport 481-A High-Performance Rotation Stage. Next to the rotation stage is another high-flatness plate used to connect the rotation stage to the bone substitute. The bone substitute is then connected to a ball bearing attached to a 2D bearing. This 2D bearing uses frictionless ball bearings to provide rotational degrees of freedom about the x-axis and the y-axis. This 2D bearing sits on top of the gold Newport DS65-Z Compact Dovetail Linear Stage. (b) The front and right views of the 2D bearing are shown. The green arrows show the rotational degrees of freedom about the x-axis and the y-axis, allowed by the ball bearings. (c) A photograph of the first prototype. The translation

stage sits on a piece of wood with acrylic on the bottom. Below the acrylic is an air table, which provides a frictionless surface.

Figure 3 shows the first prototype. This design also incorporates the three key principles. In the blue, you see the load cell attached to the high-flatness grey plate. In Figure 3c, this is the JR3 45E15 M63J load cell. The gold-colored Newport DS65-Z Compact Dovetail Linear Stage is used to apply the displacement along the z-axis, shown by the red arrow. In Figure 3c, this translation stage is black and sits on top of the wood plate. The black rotation stage allows for rotation of the bone about its neutral axis, as we measure different force data for the same displacement in 360 degrees worth of orientations. It is important to note that between the load cell and bone substitute there is a need for another high-flatness plate for the same reasons as the first high-flatness plate. Additionally, since rotation of the bone occurs about the center of the rotation stage, we also want rotation to occur about the center of the bone along the y-axis. To achieve this, the center of the high-flatness plate must be along the same axis as the center of the rotation stage. It is there where the bone substitute will be rigidly fixed to the high-flatness plate.

In the previous designs we have struggled to maintain 5 degrees of freedom (recall that those were rotation about the x-axis, rotation about the y-axis, rotation about the z-axis, translation along the x-axis and translation along the y-axis). However, in this design we have achieved this goal of maintaining all 5 degrees of freedom.

Rotation about the x-axis and rotation about the y-axis were both achieved by the 2D bearing system. This can be seen by Figure 3b. In Figure 3b, one can see an apparatus that uses three ball bearings. Specifically, those are Precision, Shielded, NO. 6001-2Z, for 12mm Shaft Diameter, part number 6661K14. These ball bearings use a grease lubricant to create frictionless rotation of the inner diameter about the outer diameter, or vice versa. In our apparatus, one ball bearing is press fit into a shaft that acts like a pin joint. It is ideally perfectly along the x-axis. This is best seen in the right view of Figure 3b. In the front view of Figure 3b, one can see the ball bearings that the bone attaches to. Ideally, these two ball bearings are perpendicular to the first one. An isometric view of this apparatus is seen in Figure 3a.

The last three degrees of freedom are achieved through the air table shown in Figure 3c. Those are rotation about the z-axis, translation along the x-axis, and translation along the y-axis. As shown in Figure 3c, the translation stage is mounted to birch wood, which is in turn mounted to a sheet of acrylic. When the air table is turned on, air is pushed out of tiny holes in the air table and below the sheet of acrylic a thin layer of air forms, thus, creating a frictionless surface between the air table and the acrylic. This can be understood through equation 2,

$$P = \frac{F}{A} \quad (2)$$

Where *P* is the pressure exerted by the air table, *F* is the weight of the apparatus on top of the air table, and *A* is the area of the acrylic sheet. Initially, it was a concern whether or not the air table would apply enough pressure to support this apparatus. However, we realized that even with an 8 x 8 in sheet of acrylic we would be able to support the weight of the translation stage and 2D bearing.

Takeaways

At the end of last semester, we instantly realized four areas in our design that we wished to improve:

1. We needed a larger translation stage. The Newport DS65-Z Compact Dovetail Linear Stage had a maximum translation of 14 mm. We quickly realized that this displacement would not be large enough to eventually test on the larger chicken bone.
2. We needed to automate the translation stage. The Newport DS65-Z Compact Dovetail Linear Stage was actuated by a manually turned thumb screw. When we turn this in between measuring data we introduce new kinematics from our hand that interfere with the 5 degrees of freedom. And as mentioned before, if we lose those degrees of freedom then we are no longer able to have the one-dimensional Hooke's Law relationship from equation 1.
3. We want a lower friction 2D rotation stage. The Precision, Shielded, NO. 6001-2Z Roller Bearings simply were not as frictionless as we wanted. It did not produce the free motion that we hoped for. Since these bearings did not allow for free motion, we could not say that these degrees of freedom (rotation about the x-axis and rotation about the y-axis) are actually free.
4. We want a more mechanically sound XY planar stage. Recall that in the first prototype, to achieve free translation along the x-axis and the y-axis, and free rotation about the z-axis, we planned to use an air table. However, as these unknown loads begin to increase on the air table it is not simple to use equation 2 to determine how large we want to make our acrylic sheet. Additionally, one can imagine that if the tested joint applies large moments, it can be enough to cause the acrylic sheet to pitch and/or roll. If this happens, the thin air layer between the acrylic sheet and the air table can be overcome, causing the acrylic sheet to touch the air table. This would produce friction. Thus, we would have lost these degrees of freedom.

These four takeaways are what motivated our design process this semester. All of these problems were adequately addressed in the final design, which will be shown in the next section.

Final Design

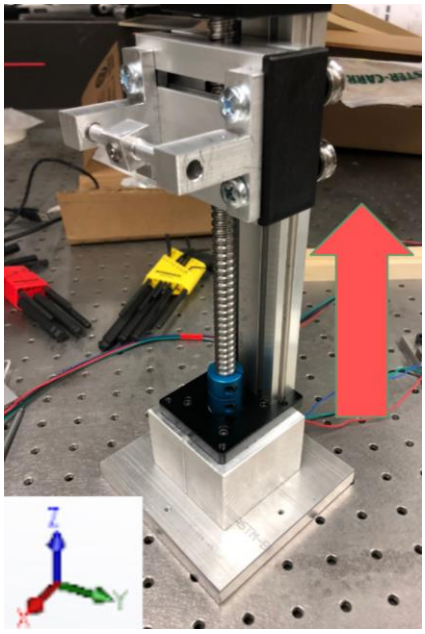

Figure 4: *A 200mm length linear rail guide, powered by a Nema 17 stepper motor. The stepper motor has a high torque of 5 kg·cm and a step precision of 1.8° per step. This translates to an accuracy of ± 0.02mm on the linear rail guide.*

We were able to address the issues presented by takeaways 1 and 2 by replacing the Newport DS65-Z Compact Dovetail Linear Stage with the 200mm linear rail guide shown in Figure 5. It is a 200mm length linear rail guide, powered by a Nema 17 stepper motor. Specifically, the stepper motor is of model number ST42H4809. The stepper motor has a maximum displacement of 200mm and is automatically actuated through the stepper motor. When given a step input, the stepper motor turns the lead screw shown in Figure 4, which in turn moves the joint either up or down along the z-axis, which imposes the previously planned displacement along the z-axis.

One downfall of this linear rail guide is that we may lose precision in measurement. The linear rail guide has an uncertainty of ±0.02mm. This is not as precise as the Newport DS65-Z Compact Dovetail Linear Stage, which is accurate up to 1 micron. However, we believe the lack in precision is replaced by the ease of use coming from automation. The stepper motor has a step angle of 1.8 degrees. Ultimately, if we aimed to automate the Newport DS65-Z Compact Dovetail Linear Stage, its accuracy would be determined by motor that would actuate it. With this new linear rail guide, we now have both a larger and automated translation stage.

One initial challenge in using this linear rail guide was trying to actuate it. The stepper motor drew both a current of 1.5 amperes and a voltage of 12 volts. Traditional Arduino motor shields do not provide this power output. To address this issue, we ordered a SMAKN® TB6600 Upgraded Version 32 Segments 4A 40V 57/86 Stepper Motor Driver, and a NEWSTYLE 24V 15A Dc Universal Regulated Switching Power Supply. Their connections can be seen in Figure 5. The Stepper Motor Driver allowed for us to use a simple Arduino to actuate the NEMA 17 Stepper Motor. The code used in the experiments moved the linear rail guide 1.092in along the z-axis. This code can be found in the Appendix.

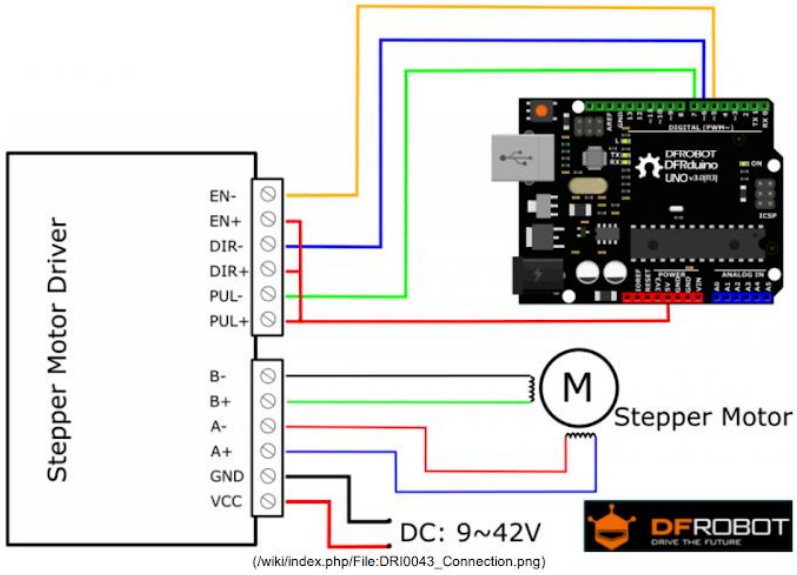

Figure 5: *Circuit schematic of the connections between the NEMA 17 Stepper Motor,* SMAKN® TB6600 Upgraded Version 32 Segments 4A 40V 57/86 Stepper Motor Driver, NEWSTYLE 24V 15A Dc Universal Regulated Switching Power Supply, and Arduino Uno used to actuate the linear rail guide.

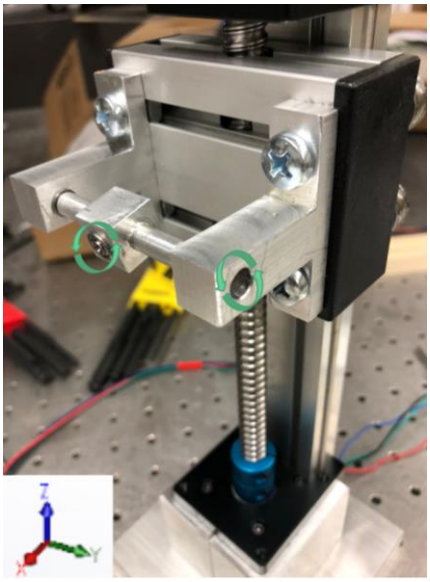

Figure 6: *This Figure shows the 2D rotation stage. It creates free rotation about both the x and y axes, shown by the green arrows. It does this using low friction* Stainless Steel Ball Bearing Flanged, Shielded with Extended Inner Ring, Number R144-2Z. Precision machining ensures that these bearings are indeed perpendicular to one another.

The third takeaway was the need for a lower friction 2D rotation stage. This can be seen in Figure 6. This 2D rotation stage serves the same purpose as the one in Figure 3, from the first prototype. It creates two rotational degrees of freedom about the x and y axes. However, we replaced the Precision, Shielded, NO. 6001-2Z Ball Bearings with Stainless Steel Ball Bearing Flanged, Shielded with Extended Inner Ring, Number R144-2Z. It was fairly well known that the smaller bearings tend to have a freer motion, and lower friction. The Stainless-Steel Ball Bearings used in the final design have a ¼ inch inner diameter and a ½ in outer diameter, as opposed to the previous bearings that were ½ in inner diameter. Furthermore, it can be seen that rotation stage that holds these bearings are machined as opposed to the 3D printed 2D rotation stage in the first prototype. Precision machining allows us to ensure that the bearings that allow for rotation about the x-axis are perfectly perpendicular to the bearings that allow for rotation about the y-axis. Additionally, we can ensure that these axes are perpendicular to the z-axis where the imposed motion is applied. This is important because as we create these free motions, we want to make sure that they are free about the correct axes (i.e. everything is aligned correctly and perpendicular to one another). Through the incorporation of this new 2D rotation stage, we now have free rotation about both the x and y axes.

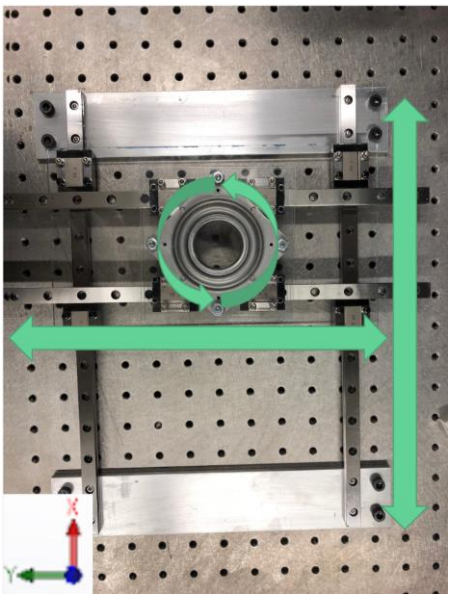

Figure 7: *The XY planar stage is shown. It allows for translation along both the x and y axes simultaneously. Additionally, it allows for rotation about the z-axis. Free translation is achieved through the use of the Corrosion-Resistant Ball Bearing Carriage, and the 12mm Wide Guide Rail for Ball Bearing Carriage. Free rotation is achieved through a 3" Inch Lazy Susan Turntable Bearing. These degrees of freedom are shown by the green arrows.*

In Figure 7, one can see the XY planar stage. It creates 3 free degrees of freedom. Nominally, those are translation along the x-axis, translation along the y-axis, and rotation about the z-axis. As mentioned in takeaway number four we wanted to create a more mechanically sound rotation stage, as problems in friction may arise due unknown moments and loads. The XY planar stage creates these three free degrees of freedom in a mechanically sound way using three layers. The first layer has 2 parallel 12mm Wide Guide Rails for Ball Bearing Carriages, and 4 Corrosion-Resistant Ball Bearing Carriages. Screwed in on top of the ball bearing carriages sits an acrylic sheet. The guide rail in combination with the acrylic sheet allow for free translation along the x-axis. The 12mm Wide Guide Rails for Ball Bearing Carriages, and Corrosion-Resistant Ball Bearing Carriages used in combination allow for very smooth, frictionless translation. The second layer again uses 2 parallel 12mm Wide Guide Rails for Ball Bearing Carriages, and 4 Corrosion-Resistant Ball Bearing Carriages. However, this time these guide rails are set perpendicular to the previous guide rail. The guide rail in layer 2 are screwed in to the acrylic sheet in layer 1. Screwed in top of the ball bearing carriages in layer 2 again sits an acrylic sheet. This sheet can now move freely along the y-axis. Lastly, in layer 3, a 3" Inch Lazy Susan Turntable Bearing has its bottom half screwed to the top of layer 2 and on its top half sits the linear rail guide shown in Figure 4. It is important to note that the sheet that the linear rail guide sits on is machined. Thus, we can have our linear rail guide placed directly in the middle of the 3" Inch Lazy Susan Turntable Bearing. With this we have established free rotation about the z-axis. Through the incorporation of this new XY planar stage, we now have a mechanically sound system that creates free translation along both the x and y axes, and free rotation about the z-axis.

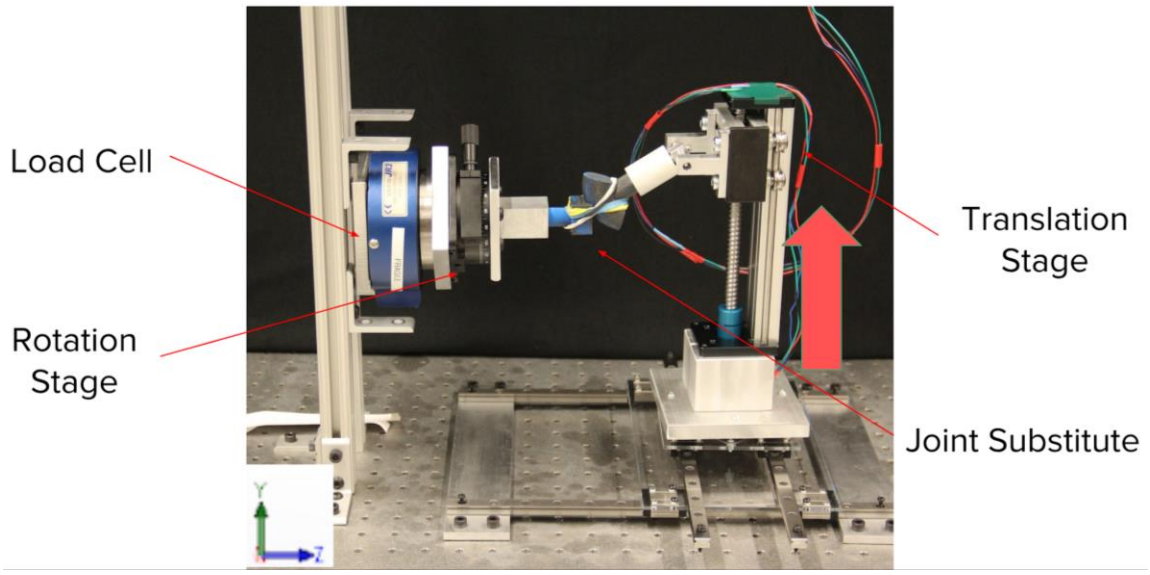

Figure 8: *The final experimental set up is shown here. The three key principles are incorporated in this experimental set-up. The translation stage applies a translation shown by the red arrow. The load cell measures a force. Then, the rotation stage can be used to accurately rotate the joint substitute. Additionally, five free degrees of freedom are produced through the use of the XY planar stage, and the 2D rotation stage. It is important to note in the bottom left hand corner there is a new coordinate axis. This coordinate axis comes from the readings that the load cell takes, which will be important in the experimental results.*

Figure 8 shows the final experimental set up. The three key principles are incorporated in this experimental set-up. The translation stage applies a translation shown by the red arrow. The load cell measures a force. Then, the rotation stage can be used to accurately rotate the joint substitute. Additionally, five free degrees of freedom are produced through the use of the XY planar stage, and the 2D rotation stage. It is important to note that in the bottom left hand corner there is a new coordinate axis. This is in relation to the readings that the load cell takes, which will be important in the experimental results. Notice that the z-direction is now horizontal on the page as opposed to vertical.

EXPERIMENTAL RESULTS

As mentioned previously, we aimed to create a mathematical relationship between the surface geometry of the joint and the directions it would move. We aimed to do this by designing an experiment that would determine the soft and stiff directions of a joint and comparing those directions to CT scans of the articular surfaces of those joints. We designed an experiment that has one imposed motion along the z-axis and has five other degrees of freedom: rotation about the x-axis, rotation about the y-axis, rotation about the z-axis, translation along the x-axis, and translation along the y-axis. The experimental set-up can be seen in Figure 8. To test the proof of concept of our design, we used a hinge joint made with Legos. Knowing the geometry of this joint allows us to take advantage of easily comparing stiffness data to the orientation the joint was in during the experiment.

The experiment can be seen in the video provided by this link: https://www.youtube.com/watch?v=ASnV038SYHY. We used the Arduino code shown in the Appendix, to actuate the linear rail guide. According to ImageJ analysis of the photos we took during the experiment, we moved the linear rail guide up 1.092 inches, then back down 1.092 inches. When the

linear rail guide was moved up (not in the neutral position), the JR3 45E15 M63J load cell took force data over an average of 10 seconds. Data collection was taken using MATLAB, and the code to do so is in the Appendix. Then the linear rail guide automatically returned to back to the neutral position. While at this neutral position, we manually turned the rotation stage 10 degrees. Then the linear rail guide was moved up 1.092 inches, data was taken, and moved down 1.092 inches, where we then rotated the rotation stage an additional 10 degrees. This process was repeated until we had force data for orientations ranging from 0 degrees to 90 degrees, in 10 degree increments. In our Lego hinge joint 0 degrees is defined as the soft direction, where the hinge is most free to move, and 90 degrees is defined as the stiff direction.

In the video it is important to note that in both the 30 degree and 60 degree orientation that there is motion on the XY planar stage This occurs due to successfully creating the 5 free degrees of freedom. As the imposed motion moves against the designed motion of the hinge the free degrees of freedom allow for the displacement the hinge is designed for. Thus, we only measure the force due to the applied displacement, and we can obtain a stiffness based on the one-dimensional Equation 1. Additionally, in the video we do not see motion of the stage when the hinge is in the 0 and 90 degree direction. This is expected. In the 0 degree direction the hinge is designed to move in the same direction as the applied displacement. In the 90 degree direction, the hinge is designed to move perpendicular to the applied displacement and thus there will be no forces causing motion on the XY planar stage. Figure 9 shows the results of the data collected in the video.

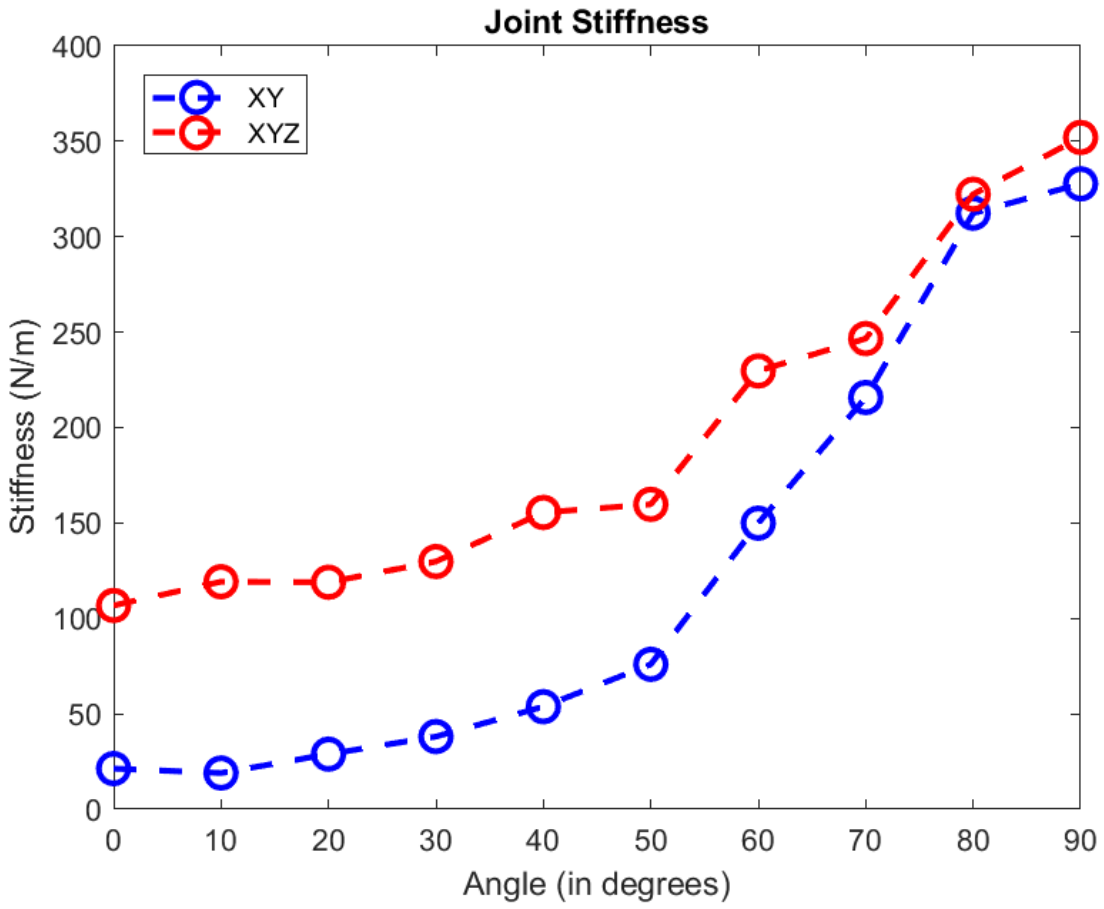

Figure 9: *A plot of stiffness, in N/m, of the joint as a function of its orientation in degrees. This data is a result of the experiment shown in the video described above. The blue line shows the stiffness measured when the force used to determine the stiffness in Equation 1 is a resultant of the x and y directions of the load cell. The red line shows the stiffness measured when the force used to determine the stiffness in Equation 1 is a resultant of the x, y, and z directions of the load cell.*

Figure 9 shows a plot of stiffness, in N/m, of the joint as a function of its orientation in degrees. As mentioned above, a JR3 45E15 M63J load cell took force data as the joint was displaced. With the known displacement of 1.094 inches, found using ImageJ of stills of the experiment, we were able to use Equation 1 to plot the stiffness as a function of angle. Intuitively, we expect stiffness to increase as the angle increases, as we go from the soft (0 degrees) to the stiff direction (90 degrees). Figure 9 displays this nicely. One thing to notice is that in Figure 9, ideally the soft direct should have zero stiffness, but we do not see this. This is not due to experimental error, rather we are measuring the friction in our hinge. This is something that we do not expect to see in the chicken knee experiment as biological joints have very low friction.

In Figure 9 there are two lines plotted. The blue line shows the stiffness measured when the force is a resultant of the x and y directions of the load cell. The red line shows the stiffness measured when the force is a resultant of the x, y, and z directions of the load cell. Since we know that the z-axis is perfectly parallel to the translation in the XY planar stage (seen in Figure 8), we expect the red and blue line to be the same, as there should be no force along the load cell's z-axis. However, this is not the case. We believe this to be due to two bad Corrosion-Resistant Ball Bearing Carriages that sit on the first layer of the XY planar stage. This difference that we are measuring is due to friction caused by these two bearings.

Additionally, it is important to note that based on the coordinate axes shown in Figure 8, We should theoretically not have any force in the x-direction. However, the axis plotted in Figure 8 are ideal. In our set up, it was not possible to position the load cell such that the x-axis was parallel to the XY planar stage. Thus, the resultant of the x and y forces must be used to calculate the stiffness due to the displacement in the linear rail guide. Theoretically, that resultant force should be parallel to the displacement imposed by the linear rail guide.

SUMMARY AND NEXT STEPS

In summary, we aimed to design an experiment to test the theory that the displacement of a joint can be determined based purely on the principal curvatures of the articular surfaces. To do this, we incorporated three key principles into the design of our experiment. First, we will apply a known displacement. Secondly, we will measure a force. Thirdly, we will rotate the joint about its neutral axis and repeat displacement and measurements until we have data about all 360 degrees of the joint. With these three key principles, we can use the one-dimensional Hooke's Law to determine a stiffness at a given orientation, and ultimately determine which directions are the soft and stiff directions of the bone. Afterwards, this data can be compared to CT scans of the joint which will be used to create a geometrical relationship between surface curvature and displacement. Ultimately, were able to obtain these three key principles. Initially, displacement was applied by a 200 mm Travel Length Linear Stage actuated by a NEMA 17 ST42H4809 Stepper Motor. Force was measured using a JR3 45E15 M63J load cell. Rotation about the neutral axis of the bone in between measurements was incorporated using the Newport 481-A High-Performance Rotation Stage.

When designing this experiment, we realized the biggest design constraint was maintaining five degrees of freedom and one imposed motion. We choose those degrees of freedom to be rotation

about the x-axis, rotation about the y-axis, rotation about the z-axis, translation along the x-axis, and translation along the y-axis. We choose the imposed motion to be translation along the z-axis. The rotational degrees of freedom about both the x-axis and the y-axis were achieved through the design of a 2D rotation stage, which through precision machining has Stainless Steel Ball Bearing Flanged, Shielded with Extended Inner Ring, Number R144-2Z aligned precisely perpendicular to each other. The translational degrees of freedom along the x-axis and the y-axis and the rotational degree of freedom about the z-axis were obtained by designing a three-layer XY planar stage. The first and second layers both use 2 parallel 12mm Wide Guide Rails for Ball Bearing Carriages, and 4 Corrosion-Resistant Ball Bearing Carriages each to provided free translation about the x-axis and y-axis respectively. The third layer uses a 3" Inch Lazy Susan Turntable Bearing to provide free rotation about the z-axis. Thus, the 2D rotation stage and the XY planar stage create five free degrees of freedom.

A SMAKN® TB6600 Upgraded Version 32 Segments 4A 40V 57/86 Stepper Motor Driver, a NEWSTYLE 24V 15A Dc Universal Regulated Switching Power Supply, and an Arduino Uno were used to actuate the NEMA 17 Stepper Motor. This in turn moved the linear rail guide 1.092in along the z-axis. As the linear rail guide was moved up along the z-axis away from its neutral position force data was taken with a JR3 45E15 M63J load cell. Using Equation 1, we were able to turn this force data into a stiffness, shown in Figure 9. As expected, when the joint was rotated closer to the stiff direction the measured stiffness increased. However, we did notice that there was considerable friction in the XY planar stage. We believe this to be due to 2 Corrosion-Resistant Ball Bearing Carriages that we noticed did not produce the same smooth motion as the others. Nevertheless, we can say the experiment was a success. Upon replacing those Corrosion-Resistant Ball Bearing Carriages, the experiment is ready to be tested on an ex vivo chicken knee.

REFERENCES

[1] Ateshian, Gerard A., et al. "Anatomically correct prosthesis and method and apparatus for manufacturing prosthesis." U.S. Patent No. 6,126,690. 3 Oct. 2000.

[2] Austin, Michael Stephen. "Anatomically correct endoluminal prostheses." U.S. Patent No. 7,722,663. 25 May 2010.

[3] Brainerd, Elizabeth L., et al. "X-ray reconstruction of moving morphology (XROMM): precision, accuracy and applications in comparative biomechanics research." Journal of Experimental Zoology Part A: Ecological and Integrative Physiology 313.5 (2010): 262-279.

[4] Carrano, Matthew T., and John R. Hutchinson. "Pelvic and hindlimb musculature of Tyrannosaurus rex (Dinosauria: Theropoda)." Journal of Morphology 253.3 (2002): 207-228.

[5] Doube, Michael, et al. "BoneJ: free and extensible bone image analysis in ImageJ." Bone 47.6 (2010): 1076-1079.

[6] Grood, E. S., & Suntay, W. J. (1983). A joint coordinate system for the clinical description of three-dimensional motions: application to the knee. *Journal of biomechanical engineering*, *105*(2), 136-144.

[7] Karduna, Andrew R., et al. "Kinematics of the glenohumeral joint: influences of muscle forces, ligamentous constraints, and articular geometry." Journal of Orthopaedic Research 14.6 (1996): 986-993.

[8] Kelkar, Rajeev, et al. "Glenohumeral mechanics: a study of articular geometry, contact, and kinematics." Journal of Shoulder and Elbow Surgery 10.1 (2001): 73-84.

[9] "Ligament." *Wikipedia*. Wikimedia Foundation, 16 Dec. 2017. Web. 19 Dec. 2017.

[10] Marzke, Mary W., and Robert F. Marzke. "Evolution of the human hand: approaches to acquiring, analysing and interpreting the anatomical evidence." *The Journal of Anatomy*197.1 (2000): 121-140.

[11] Marzke, Mary W., et al. "Comparative 3D quantitative analyses of trapeziometacarpal joint surface curvatures among living catarrhines and fossil hominins." *American Journal of Physical Anthropology* 141.1 (2010): 38-51.

[12] Santos, V. J., & Valero-Cuevas, F. J. (2006). Reported anatomical variability naturally leads to multimodal distributions of Denavit-Hartenberg parameters for the human thumb. *IEEE Transactions on Biomedical Engineering*, *53*(2), 155-163.

[13] "Stiffness." *Wikipedia*. Wikimedia Foundation, 06 Nov. 2017. Web. 19 Dec. 2017.

[14] Van Veen, S. (2013). *Planar Ferrofluid Bearings* (Master's thesis). Retrieved from http://repository.tudelft.nl/

APPENDIX

Arduino Code for Linear Rail Guide

```
int PUL=7; //define Pulse pin
int DIR=6; //define Direction pin
int ENA=5; //define Enable Pin
int step = 0;

void setup() {
pinMode (PUL, OUTPUT);
pinMode (DIR, OUTPUT);
pinMode (ENA, OUTPUT);
Serial.begin(9600);
}

void loop() {
for (int i=0; i<30000; i++) //Forward
{
digitalWrite(DIR,LOW);
digitalWrite(ENA,HIGH);
digitalWrite(PUL,HIGH);
delayMicroseconds(50);
digitalWrite(PUL,LOW);
delayMicroseconds(50);
}
delay(10);
for (int i=0; i<15000; i++) //Forward
{
digitalWrite(DIR,LOW);
```

```
digitalWrite(ENA,HIGH);
digitalWrite(PUL,HIGH);
delayMicroseconds(50);
digitalWrite(PUL,LOW);
delayMicroseconds(50);
}
delay(20000);
for (int i=0; i<30000; i++) //Backward
{
digitalWrite(DIR,HIGH);
digitalWrite(ENA,HIGH);
digitalWrite(PUL,HIGH);
delayMicroseconds(50);
digitalWrite(PUL,LOW);
delayMicroseconds(50);
}
delay(10);
for (int i=0; i<15000; i++) //Backward
{
digitalWrite(DIR,HIGH);
digitalWrite(ENA,HIGH);
digitalWrite(PUL,HIGH);
delayMicroseconds(50);
digitalWrite(PUL,LOW);
delayMicroseconds(50);
}
delay(45000);
}
```

MATLAB Code for JR3 45E15 M63J Load Cell Data Collection

```
clear all
close all

s=daq.createSession('ni');
Channels = addAnalogInputChannel(s,'Dev1',[8,1,9,10,0,2],'Voltage');

savedData = zeros(10,6);

% in = {'ai1','ai2','ai3','ai4','ai5','ai6'};
for i=1:6
    Channels(i).InputType = 'SingleEnded';
    Channels(i).Range = [-5 5];
end

tend=10;
s.Rate = 2000;
s.DurationInSeconds = tend;

disp('Do not touch the load cell.')

[data] = s.startForeground;
data=data(:,1:6);

% Calibration matrix for the load cell
cal=[26.337,-0.158,0.286,-0.681,-0.464,0.224;...
    0.193,26.893,0.162,-0.447,-0.534,-0.859;...
    -1.198, 1.584, 53.006, -0.041,-0.408,-3.533;...
    0.067,-0.007,0.003,3.295,-0.004,0.126;...
    -0.018,0.000,-0.002,0.003,3.397,-0.104;...
    -0.012,-0.001,0.004,-0.012,0.002,3.278];

fmdata=data*cal;
meandata = mean(fmdata, 1);
% save('data.csv','meandata','-ASCII')
```

MATLAB Code for to Produce Stiffness Calculations

```
clear all
close all

xData = 3.959 - 2.867; %displacement found using imageJ in inches
xData = 0.0254*xData; %convert inches to meter

%initialize vaiables
kData = ones(1,10);
kDataZ = ones(1,10);
checkData = ones(10,6); %check to see if fz, mx, my, mz are zero.
```

```
for i = 0:10:90
   data0 = load(['data0_',int2str(i),'.csv']); %load zero data
   data = load(['data_',int2str(i),'.csv']); %load force data
   data = data - data0; %remove the zero calibration
   fData = sqrt(data(1)^2+data(2)^2); %Calculate the Force
   fDataZ = sqrt(data(1)^2+data(2)^2+data(3)^2); %Calculate the Force
with Z direction included
   kData(i/10+1) = fData/xData; %Calculate the stiffness
   kDataZ(i/10+1) = fDataZ/xData; %Calculate the stiffness with Z
direction included
   checkData(i/10+1,:) = data(1:6); %check to see if fz, mx, my, mz
are zero.
end

% check to see if moments are zero
disp('       Fx       Fy       Fz       Mx          My       Mz');
disp(checkData);

% Graph
angle =  [0:10:90];
plot(angle, kData, 'b--o', 'MarkerSize', 10, 'LineWidth', 2); hold on;
plot(angle, kDataZ, 'r--o', 'MarkerSize', 10, 'LineWidth', 2); hold
on;
xlabel({'Angle (in degrees)'});
ylabel('Stiffness (N/m)');
title('Joint Stiffness');
legend('XY', 'XYZ','Location','northwest');
saveas(gcf, 'hingeJoint.png');

%% graph the moments
figure;
plot(angle, checkData(:,4),'b--o', 'MarkerSize', 10, 'LineWidth', 2);
hold on;
plot(angle, checkData(:,5),'r--o', 'MarkerSize', 10, 'LineWidth', 2);
hold on;
plot(angle, checkData(:,6),'y--o', 'MarkerSize', 10, 'LineWidth', 2);
hold on;
xlabel({'Angle (in degrees)'});
ylabel('Moment (N.m)');
title('Measured Moments');
legend('X','Y','Z','Location','northwest');
saveas(gcf, 'hingeJointMoments.png');
```